Evidence for the baryonic decay $\overline{B}^0 \to D^0 \Lambda \overline{\Lambda}$

Laboratoire d'Annecy-le-Vieux de Physique des Particules (LAPP), Université de Savoie, CNRS/IN2P3, F-74941 Annecy-Le-Vieux, France

Universitat de Barcelona, Facultat de Fisica, Departament ECM, E-08028 Barcelona, Spain

INFN Sezione di Bari[a]; Dipartimento di Fisica, Università di Bari[b], I-70126 Bari, Italy

University of Bergen, Institute of Physics, N-5007 Bergen, Norway

Lawrence Berkeley National Laboratory and University of California, Berkeley, California 94720, USA

Ruhr Universität Bochum, Institut für Experimentalphysik 1, D-44780 Bochum, Germany

University of British Columbia, Vancouver, British Columbia, Canada V6T 1Z1

Brunel University, Uxbridge, Middlesex UB8 3PH, United Kingdom

Budker Institute of Nuclear Physics SB RAS, Novosibirsk 630090[a], Novosibirsk State University, Novosibirsk 630090[b], Novosibirsk State Technical University, Novosibirsk 630092[c], Russia

University of California at Irvine, Irvine, California 92697, USA

University of California at Riverside, Riverside, California 92521, USA

University of California at Santa Barbara, Santa Barbara, California 93106, USA

University of California at Santa Cruz, Institute for Particle Physics, Santa Cruz, California 95064, USA

California Institute of Technology, Pasadena, California 91125, USA

University of Cincinnati, Cincinnati, Ohio 45221, USA

University of Colorado, Boulder, Colorado 80309, USA

Colorado State University, Fort Collins, Colorado 80523, USA

Technische Universität Dortmund, Fakultät Physik, D-44221 Dortmund, Germany

Technische Universität Dresden, Institut für Kern- und Teilchenphysik, D-01062 Dresden, Germany

Laboratoire Leprince-Ringuet, Ecole Polytechnique, CNRS/IN2P3, F-91128 Palaiseau, France

University of Edinburgh, Edinburgh EH9 3JZ, United Kingdom

INFN Sezione di Ferrara[a]; Dipartimento di Fisica e Scienze della Terra, Università di Ferrara[b], I-44122 Ferrara, Italy

INFN Laboratori Nazionali di Frascati, I-00044 Frascati, Italy

INFN Sezione di Genova[a]; Dipartimento di Fisica, Università di Genova[b], I-16146 Genova, Italy

Indian Institute of Technology Guwahati, Guwahati, Assam, 781 039, India

Harvard University, Cambridge, Massachusetts 02138, USA

Universität Heidelberg, Physikalisches Institut, D-69120 Heidelberg, Germany

Humboldt-Universität zu Berlin, Institut für Physik, D-12489 Berlin, Germany

Imperial College London, London, SW7 2AZ, United Kingdom

University of Iowa, Iowa City, Iowa 52242, USA

Iowa State University, Ames, Iowa 50011-3160, USA

Johns Hopkins University, Baltimore, Maryland 21218, USA

Laboratoire de l'Accélérateur Linéaire, IN2P3/CNRS et Université Paris-Sud 11, Centre Scientifique d'Orsay, F-91898 Orsay Cedex, France

Lawrence Livermore National Laboratory, Livermore, California 94550, USA

University of Liverpool, Liverpool L69 7ZE, United Kingdom

Queen Mary, University of London, London, E1 4NS, United Kingdom

University of London, Royal Holloway and Bedford New College, Egham, Surrey TW20 0EX, United Kingdom

University of Louisville, Louisville, Kentucky 40292, USA

Johannes Gutenberg-Universität Mainz, Institut für Kernphysik, D-55099 Mainz, Germany

University of Manchester, Manchester M13 9PL, United Kingdom

University of Maryland, College Park, Maryland 20742, USA

Massachusetts Institute of Technology, Laboratory for Nuclear Science, Cambridge, Massachusetts 02139, USA

McGill University, Montréal, Québec, Canada H3A 2T8

INFN Sezione di Milano[a]; Dipartimento di Fisica, Università di Milano[b], I-20133 Milano, Italy

University of Mississippi, University, Mississippi 38677, USA

Université de Montréal, Physique des Particules, Montréal, Québec, Canada H3C 3J7

INFN Sezione di Napoli[a]; Dipartimento di Scienze Fisiche,
Università di Napoli Federico II[b], I-80126 Napoli, Italy

NIKHEF, National Institute for Nuclear Physics and High Energy Physics, NL-1009 DB Amsterdam, The Netherlands

University of Notre Dame, Notre Dame, Indiana 46556, USA

Ohio State University, Columbus, Ohio 43210, USA

University of Oregon, Eugene, Oregon 97403, USA

INFN Sezione di Padova[a]; Dipartimento di Fisica, Università di Padova[b], I-35131 Padova, Italy

Laboratoire de Physique Nucléaire et de Hautes Energies,
IN2P3/CNRS, Université Pierre et Marie Curie-Paris6,

Université Denis Diderot-Paris7, F-75252 Paris, France

INFN Sezione di Perugia[a]; Dipartimento di Fisica, Università di Perugia[b], I-06123 Perugia, Italy

INFN Sezione di Pisa[a]; Dipartimento di Fisica, Università di Pisa[b]; Scuola Normale Superiore di Pisa[c], I-56127 Pisa, Italy

Princeton University, Princeton, New Jersey 08544, USA

INFN Sezione di Roma[a]; Dipartimento di Fisica,
Università di Roma La Sapienza[b], I-00185 Roma, Italy

Universität Rostock, D-18051 Rostock, Germany

Rutherford Appleton Laboratory, Chilton, Didcot, Oxon, OX11 0QX, United Kingdom

CEA, Irfu, SPP, Centre de Saclay, F-91191 Gif-sur-Yvette, France

SLAC National Accelerator Laboratory, Stanford, California 94309 USA

University of South Carolina, Columbia, South Carolina 29208, USA

Southern Methodist University, Dallas, Texas 75275, USA

Stanford University, Stanford, California 94305-4060, USA

State University of New York, Albany, New York 12222, USA

Tel Aviv University, School of Physics and Astronomy, Tel Aviv, 69978, Israel

University of Tennessee, Knoxville, Tennessee 37996, USA

University of Texas at Austin, Austin, Texas 78712, USA

University of Texas at Dallas, Richardson, Texas 75083, USA

INFN Sezione di Torino[a]; Dipartimento di Fisica, Università di Torino[b], I-10125 Torino, Italy

INFN Sezione di Trieste[a]; Dipartimento di Fisica, Università di Trieste[b], I-34127 Trieste, Italy

IFIC, Universitat de Valencia-CSIC, E-46071 Valencia, Spain

University of Victoria, Victoria, British Columbia, Canada V8W 3P6

Department of Physics, University of Warwick, Coventry CV4 7AL, United Kingdom

University of Wisconsin, Madison, Wisconsin 53706, USA

BABAR

PACS numbers: 13.25.Hw, 13.60.Rj, 14.20.Lq

Now at the University of Tabuk, Tabuk 71491, Saudi Arabia

Also with Università di Perugia, Dipartimento di Fisica, Perugia, Italy

Now at Laboratoire de Physique Nucláire et de Hautes Energies, IN2P3/CNRS, Paris, France

Now at the University of Huddersfield, Huddersfield HD1 3DH, UK

Deceased

Now at University of South Alabama, Mobile, Alabama 36688, USA

Also with Università di Sassari, Sassari, Italy

Also with INFN Sezione di Roma, Roma, Italy

Now at Universidad Técnica Federico Santa Maria, Valparaiso, Chile 2390123

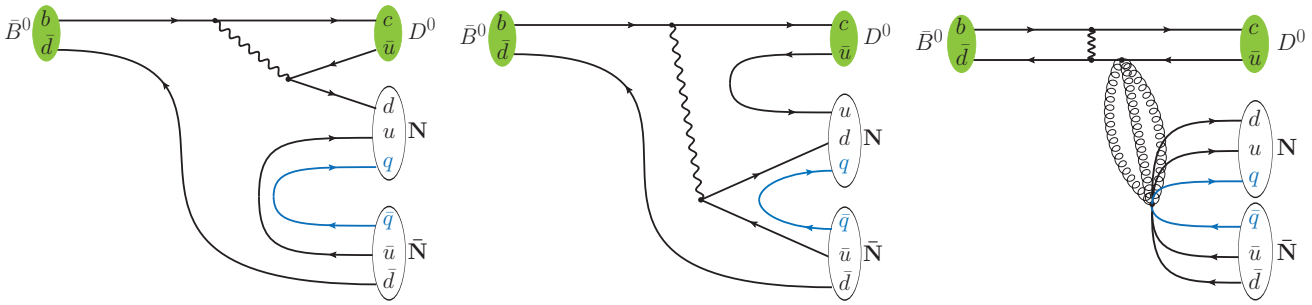

Λ **D^0**

$\bar{B}^0$

BABAR

BABAR

t

t

BABAR

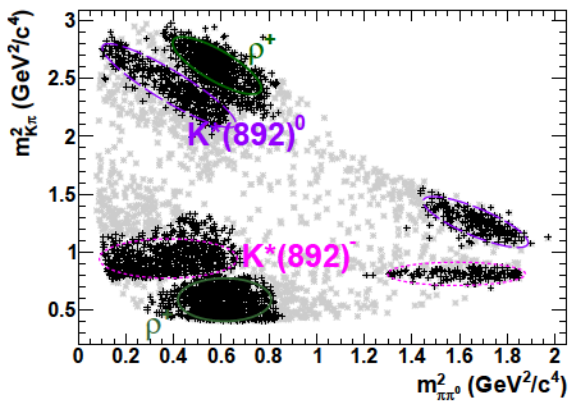

FIG. 2: Dalitz plot for simulated $D^0 \to K^-\pi^+\pi^0$ events before (gray stars) and after (black crosses) the $w_{\rm Dalitz} > 0.02$ requirement. Resonant decays are indicated.

quirement.

The D^0 and Λ candidates are constrained to their nominal masses in the reconstruction of the $\overline{B}^0$ candidates. We apply a fit to the entire decay chain and require the probability for the vertex fit to be larger than 0.001.

To reduce background from $e^+e^- \to q\overline{q}$ events with $q = u, d, s, c$, we apply a selection on a Fisher discriminant $\mathcal{F}$ that combines the values of $|\cos\theta_{\rm Thr}|$, where $\theta_{\rm Thr}$ is the angle between the thrust axis of the B candidate and the thrust axis formed from the remaining tracks and clusters in the event; $|\cos\theta_z|$, where θ_z is the angle between the B thrust axis and the beam axis; $|\cos\phi|$, where ϕ is the angle between the B momentum and the beam axis; and the normalized second Fox Wolfram moment [22]. All these quantities are defined in the center-of-mass frame. All selection criteria are summarized in Table I.

TABLE I: Summary of selection criteria.

Selection criterion	Selected candidates
$\Lambda/\overline{\Lambda}$ mass	$m_{p\pi} \in [1.112, 1.120]\,{\rm GeV}/c^2$
Flight significance	$L_t/\sigma_{L_t} > 4$
$D^0 \to K^-\pi$ mass	$m_{K\pi} \in [1.846, 1.882]\,{\rm GeV}/c^2$
$D^0 \to K^-\pi^+\pi^+\pi^-$ mass	$m_{K\pi\pi\pi} \in [1.852, 1.876]\,{\rm GeV}/c^2$
Lateral parameter γ_1	$0.05 < {\rm LAT}(\gamma_1) < 0.55$
Lateral parameter γ_2	${\rm LAT}(\gamma_2) > 0.075$
Calorimeter energy γ_1	$E(\gamma_1) > 0.125\,{\rm GeV}$
Calorimeter energy γ_2	$E(\gamma_2) > 0.04\,{\rm GeV}$
π^0 mass	$m_{\gamma\gamma} \in [0.116, 0.145]\,{\rm GeV}/c^2$
$D^0 \to K^-\pi^+\pi^0$ mass	$m_{K\pi\pi^0} \in [1.81, 1.89]\,{\rm GeV}/c^2$
Dalitz weight	$w_{\rm Dalitz} > 0.02$
B vertex probability	$p(B) > 0.001$
Fisher discriminant	$\mathcal{F} > 0.1$

IV. FIT STRATEGY

We determine the number of signal candidates with a two-dimensional unbinned extended maximum likelihood fit to the invariant mass $m(D^0\Lambda\overline{\Lambda})$ and the energy substituted mass $m_{\rm ES}$. The latter is defined as

$$m_{\rm ES} = \sqrt{(s/2 + \boldsymbol{p}_0 \cdot \boldsymbol{p}_B)^2/E_0^2 - |\boldsymbol{p}|_B^2}\,, \qquad (2)$$

where $\sqrt{s}$ is the center-of-mass energy, $\boldsymbol{p}_B$ the B candidate's momentum, and $(E_0, \boldsymbol{p}_0)$ the four-momentum vector of the e^+e^- system, each given in the laboratory frame. Both $m(D^0\Lambda\overline{\Lambda})$ and $m_{\rm ES}$ are centered at the B mass for well reconstructed B decays.

Due to the small mass difference of $76.9\,{\rm MeV}/c^2$ [1] between the Λ and Σ^0 baryons, $\overline{B}^0 \to D^0\Sigma^0\overline{\Lambda}$ decays, where the Σ^0 decays radiatively as $\Sigma^0 \to \Lambda\gamma$, are a source of background. Such events peak at the B mass in $m_{\rm ES}$ and are slightly shifted in $m(D^0\Lambda\overline{\Lambda})$ with respect to $\overline{B}^0 \to D^0\Lambda\overline{\Lambda}$ (Fig. 3). We account for this decay by including an explicit term in the likelihood function (see below), whose yield is determined in the fit.

We divide the data sample into three subsamples corresponding to the D^0 decay modes. Given their different signal-to-background ratios, we determine the number of signal candidates in a simultaneous fit to the three independent subsamples. We describe each $\overline{B}^0 \to D^0\Lambda\overline{\Lambda}$ signal sample with the product of a Novosibirsk function in $m_{\rm ES}$ and a sum of two Gaussian functions $f^{\mathcal{GG}}$ in $m(D^0\Lambda\overline{\Lambda})$ assuming that $m_{\rm ES}$ and $m(D^0\Lambda\overline{\Lambda})$ are not correlated. We study simulated samples of signal and background events and find no significant correlation between $m_{\rm ES}$ and $m(D^0\Lambda\overline{\Lambda})$. The Novosibirsk function is defined as

$$f^{\rm Novo}(m_{\rm ES}) = \exp\left[-\frac{1}{2}\left(\frac{\ln^2[1+\lambda\alpha(m_{\rm ES}-\mu)]}{\alpha^2} + \alpha^2\right)\right],$$
$$\lambda = \sinh(\alpha\sqrt{\ln 4})/(\sigma\alpha\sqrt{\ln 4}), \qquad (3)$$

with μ the mean value, σ the width, and α the tail parameter. The decay $\overline{B}^0 \to D^0\Sigma^0\overline{\Lambda}$ is described by the product of a Novosibirsk $f^{{\rm Novo1},\Sigma^0}$ function in $m_{\rm ES}$ and a sum of another Novosibirsk function $f^{{\rm Novo2},\Sigma^0}$ and a Gaussian $\mathcal{G}^{\Sigma^0}$ in $m(D^0\Lambda\overline{\Lambda})$. All parameters are determined using Monte Carlo simulated events and are fixed in the final fit. Background from $e^+e^- \to q\overline{q}$ events and other B meson decays is modeled by the product of an ARGUS function [23] in $m_{\rm ES}$ and a first order polynomial in $m(D^0\Lambda\overline{\Lambda})$.

The full fit function is defined as

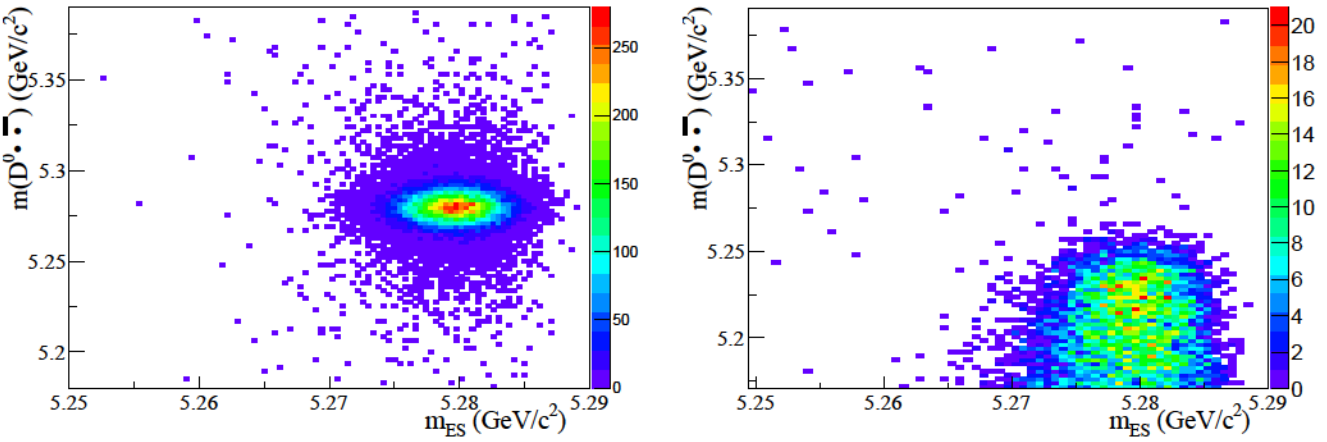

FIG. 3: Distributions for $\overline{B}^0 \to D^0 \Lambda \overline{\Lambda}$ (left) and $\overline{B}^0 \to D^0 \Sigma^0 \overline{\Lambda}$ reconstructed as $\overline{B}^0 \to D^0 \Lambda \overline{\Lambda}$ (right) for the $D^0 \to K^- \pi^+$ mode in simulated events.

$$\begin{aligned} f_j^{\rm Fit} &= f_j^{\Lambda} + f_j^{\Sigma^0} + f_j^{\rm Bkg} \\ &= f_j^{{\rm Novo},\Lambda}(m_{\rm ES}) \times f_j^{\mathcal{GG}}\left(m(D^0\Lambda\overline{\Lambda})\right) + f_j^{{\rm Novo1},\Sigma^0}(m_{\rm ES}) \times \left[f_j^{{\rm Novo2},\Sigma^0}\left(m(D^0\Lambda\overline{\Lambda})\right) + \mathcal{G}_j^{\Sigma^0}\left(m(D^0\Lambda\overline{\Lambda})\right)\right] \\ &+ f_j^{\rm ARGUS}(m_{\rm ES}) \times f_j^{\rm Poly}\left(m(D^0\Lambda\overline{\Lambda})\right), \end{aligned} \tag{4}$$

where the index j corresponds to the three D^0 decay modes.

The branching fraction is determined from

$$\begin{aligned} \mathcal{B}(\overline{B}^0 \to D^0\Lambda\overline{\Lambda}) = &\frac{N(\overline{B}^0 \to D^0\Lambda\overline{\Lambda})}{2N_{B^0\overline{B}^0} \times \varepsilon^{\Lambda}} \\ &\times \frac{1}{\mathcal{B}(\Lambda\to p\pi)^2\mathcal{B}(D^0\to X)}, \end{aligned} \tag{5}$$

where $N(\overline{B}^0 \to D^0\Lambda\overline{\Lambda})$ is the fitted signal yield, $N_{B^0\overline{B}^0}$ the number of the $B^0\overline{B}^0$ pairs assuming $\mathcal{B}(\Upsilon(4S)\to B^0\overline{B}^0) = 0.5$, ε^{Λ} the total reconstruction efficiency, and $\mathcal{B}(\Lambda\to p\pi)$ and $\mathcal{B}(D^0\to X)$ the branching fractions for the daughter decays of Λ and D^0, respectively. An analogous expression holds for $\mathcal{B}(\overline{B}^0 \to D^0\Sigma^0\overline{\Lambda})$. We perform a simultaneous fit of the three D^0 decay channels to obtain:

$$\begin{aligned} N_{\Lambda} &= \frac{N(\overline{B}^0 \to D^0\Lambda\overline{\Lambda})}{\varepsilon^{\Lambda}\mathcal{B}(D^0\to X)}, \\ N_{\Sigma^0} &= \frac{N(\overline{B}^0 \to D^0\Sigma^0\overline{\Lambda})}{\varepsilon^{\Sigma^0}\mathcal{B}(D^0\to X)}. \end{aligned} \tag{6}$$

The likelihood function is given by

$$\begin{aligned} L = \prod_j \frac{e^{-\left(\varepsilon_j^{\Lambda}\mathcal{B}_j N_{\Lambda} + N_j^{\rm Bkg} + \varepsilon_j^{\Sigma^0}\mathcal{B}_j N_{\Sigma^0}\right)}}{N(j)!} \prod_k^{N(j)} \Big[&\varepsilon_j^{\Lambda}\mathcal{B}_j N_{\Lambda} f_j^{\Lambda}\left(m_{{\rm ES}k}, m(D^0\Lambda\overline{\Lambda})_k\right) + N_j^{\rm Bkg} f_j^{\rm Bkg}\left(m_{{\rm ES}k}, m(D^0\Lambda\overline{\Lambda})_k\right) \\ &+ \varepsilon_j^{\Sigma^0}\mathcal{B}_j N_{\Sigma^0} f_j^{\Sigma^0}\left(m_{{\rm ES}k}, m(D^0\Lambda\overline{\Lambda})_k\right)\Big], \end{aligned} \tag{7}$$

where $\mathcal{B}_j$ is the branching fraction for the jth D^0 decay, $N_j^{\rm Bkg}$ the number of combinatorial background events in the jth subsample, N_{Λ} and N_{Σ^0} the yields of $\overline{B}^0 \to D^0\Lambda\overline{\Lambda}$ and $\overline{B}^0 \to D^0\Sigma^0\overline{\Lambda}$, and ε_j^{Λ} and $\varepsilon_j^{\Sigma^0}$ the efficiencies for the jth D^0 decay.

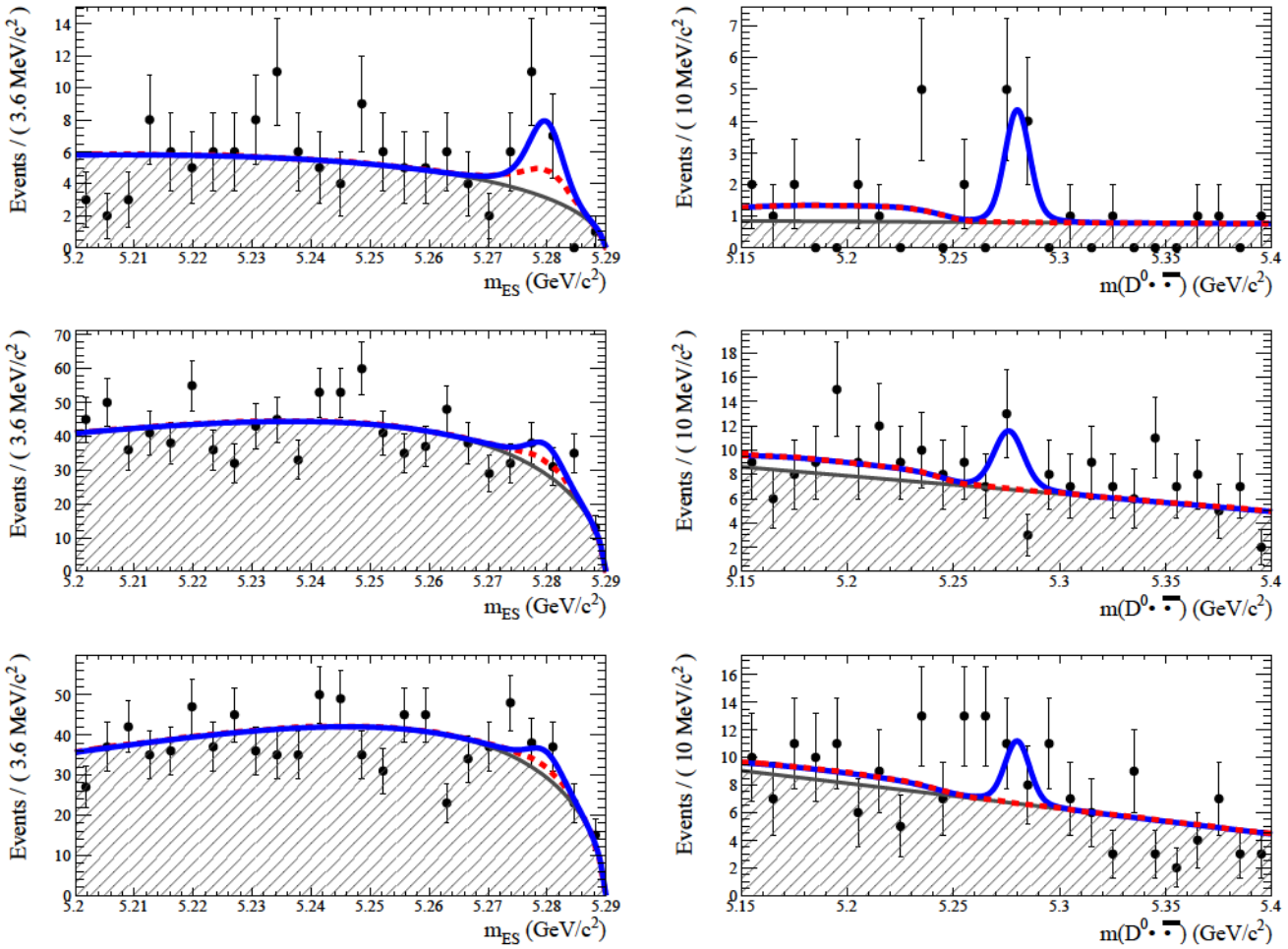

FIG. 4: Results of the combined fit. The $m_{\rm ES}$ projection is shown for $m(D^0\Lambda\overline{\Lambda}) \in [5.15, 5.31]\,{\rm GeV}/c^2$ and the $m(D^0\Lambda\overline{\Lambda})$ projection for $m_{\rm ES} \in [5.272, 5.286]\,{\rm GeV}/c^2$. The solid line shows the result of the fit, the dashed curve indicates the $\overline{B}^0 \to D^0\Sigma^0\overline{\Lambda}$ contribution, and the shaded histogram the combinatorial background. From top to bottom: $D^0 \to K^-\pi^+$, $D^0 \to K^-\pi^+\pi^0$, and $D^0 \to K^-\pi^+\pi^+\pi^-$ subsamples.

To investigate the threshold dependence, we perform the fit in bins of $m(\Lambda\overline{\Lambda})$ and examine the resulting distribution after accounting for the reconstruction efficiency and D^0 branching fractions. The results are shown in Fig. 5. No enhancement in the $\overline{B}^0 \to D^0\Lambda\overline{\Lambda}$ event rate is observed at the baryon-antibaryon mass threshold within the uncertainties, in contrast to $\overline{B}^0 \to D^0 p\overline{p}$ decays, which do exhibit such an enhancement [8].

We compare our results for the $\overline{B}^0 \to D^0\Lambda\overline{\Lambda}$ and $\overline{B}^0 \to D^0\Sigma^0\overline{\Lambda}$ branching fractions to theoretical predictions. The result we obtain for the $\overline{B}^0 \to D^0\Sigma^0\overline{\Lambda}$ branching fraction is consistent with the prediction of $\mathcal{B}(\overline{B}^0 \to D^0\Sigma^0\overline{\Lambda} + \overline{B}^0 \to D^0\Lambda\overline{\Sigma}^0) = (18 \pm 5) \times 10^{-6}$ from Ref. [11]. However, the obtained result for the $\overline{B}^0 \to D^0\Lambda\overline{\Lambda}$ branching fraction is larger than the prediction of $\mathcal{B}(\overline{B}^0 \to D^0\Lambda\overline{\Lambda}) = (2 \pm 1) \times 10^{-6}$ [11] by a factor of

$$\frac{\mathcal{B}(\overline{B}^0 \to D^0\Lambda\overline{\Lambda})_{\rm exp}}{\mathcal{B}(\overline{B}^0 \to D^0\Lambda\overline{\Lambda})_{\rm theo}} = 4.9 \pm 3.0. \qquad (11)$$

We further determine

$$\frac{\mathcal{B}(\overline{B}^0 \to D^0\Sigma^0\overline{\Lambda} + \overline{B}^0 \to D^0\Lambda\overline{\Sigma}^0)}{\mathcal{B}(\overline{B}^0 \to D^0\Lambda\overline{\Lambda})} = 1.5 \pm 0.9, \qquad (12)$$

which is in agreement with our assumption that all four modes $\overline{B}^0 \to D^0\Lambda\overline{\Lambda}$, $\overline{B}^0 \to D^0\Sigma^0\overline{\Lambda}$, $\overline{B}^0 \to D^0\Lambda\overline{\Sigma}^0$, and $\overline{B}^0 \to D^0\Sigma^0\overline{\Sigma}^0$ are produced at equal rates. For the ratio of branching fractions we find

$$\frac{\mathcal{B}(\overline{B}^0 \to D^0\Lambda\overline{\Lambda})}{\mathcal{B}(\overline{B}^0 \to D^0 p\overline{p})} = \frac{1}{10.6 \pm 3.7}, \qquad (13)$$

using $\mathcal{B}(\overline{B}^0 \to D^0 p\overline{p}) = (1.04 \pm 0.04) \times 10^{-4}$ [1]. This is in agreement with the expected suppression of 1/12 discussed in the introduction.

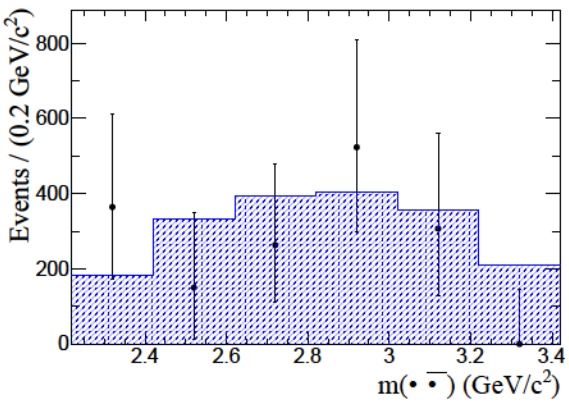

FIG. 5: Distribution of the invariant baryon-antibaryon mass for D^0-branching-fraction and efficiency-corrected $\overline{B}^0 \to D^0\Lambda\overline{\Lambda}$ signal candidates. The data points represent the *BABAR* data and the shaded histogram indicates phase-space-distributed simulated events, scaled to match the area under the data.

VII. SUMMARY

We find evidence for the baryonic B decay $\overline{B}^0 \to D^0\Lambda\overline{\Lambda}$. We determine the branching fraction to be $\mathcal{B}(\overline{B}^0 \to D^0\Lambda\overline{\Lambda}) = (9.8^{+2.9}_{-2.6} \pm 1.9) \times 10^{-6}$ with a significance of 3.4σ including systematic uncertainties. This is in agreement with the Belle measurement [13]. We find no evidence for an enhancement in the invariant baryon-antibaryon mass distribution near threshold. Our result for the branching fraction deviates from theoretical predictions based on measurements of $\overline{B}^0 \to D^0 p\overline{p}$ but agrees with simple models of hadronization. We find no evidence for the decay $\overline{B}^0 \to D^0\Sigma^0\overline{\Lambda}$ and calculate a Bayesian upper limit at 90% confidence level of $\mathcal{B}(\overline{B}^0 \to D^0\Sigma^0\overline{\Lambda} + \overline{B}^0 \to D^0\Lambda\overline{\Sigma}^0) < 3.1 \times 10^{-5}$. This result is in agreement with the theoretical expectation.

We are grateful for the extraordinary contributions of our PEP-II colleagues in achieving the excellent luminosity and machine conditions that have made this work possible. The success of this project also relies critically on the expertise and dedication of the computing organizations that support *BABAR*. The collaborating institutions wish to thank SLAC for its support and the kind hospitality extended to them. This work is supported by the US Department of Energy and National Science Foundation, the Natural Sciences and Engineering Research Council (Canada), the Commissariat à l'Energie Atomique and Institut National de Physique Nucléaire et de Physique des Particules (France), the Bundesministerium für Bildung und Forschung and Deutsche Forschungsgemeinschaft (Germany), the Istituto Nazionale di Fisica Nucleare (Italy), the Foundation for Fundamental Research on Matter (The Netherlands), the Research Council of Norway, the Ministry of Education and Science of the Russian Federation, Ministerio de Ciencia e Innovación (Spain), and the Science and Technology Facilities Council (United Kingdom). Individuals have received support from the Marie-Curie IEF program (European Union), the A. P. Sloan Foundation (USA) and the Binational Science Foundation (USA-Israel).

[1] J. Beringer *et al.* (Particle Data Group), Phys. Rev. D **86**, 010001 (2012) and 2013 partial update for the 2014 edition.
[2] D. S. Carlstone, S. P. Rosen, and S. Pakvasa, Phys. Lett. **174**, 18771881 (1968).
[3] N. Gabychev *et al.* (Belle Collaboration), Phys. Rev. Lett. **97**, 242001 (2006).
[4] B. Aubert *et al.* (*BABAR* Collaboration), Phys. Rev. D **78**, 112003 (2008).
[5] B. Aubert *et al.* (*BABAR* Collaboration), Phys. Rev. D **72**, 051101 (2005).
[6] J.T. Wei *et al.* (Belle Collaboration), Phys. Lett. B **659**, 80 (2008).
[7] R. Aaij *et al.* (LHCb Collaboration), Phys. Rev. D **88**, 052015 (2013)
[8] P. del Amo Sanchez *et al.* (*BABAR* Collaboration), Phys. Rev. D **85**, 092017 (2012).
[9] K. Abe *et al.* (Belle Collaboration), Phys. Rev. Lett. **89**, 151802 (2002).
[10] C.H. Chen *et al.*, Phys. Rev. D **78**, 054016 (2008).
[11] Y.K. Hsiao, Int. J. Mod. Phys. A **24**, 3638 (2009).
[12] G. Lafferty, J. Phys. G **23**, 731 (1997).
[13] Y.W. Chang *et al.* (Belle Collaboration), Phys. Rev. D **79**, 052006 (2009).
[14] J. P. Lees *et al.* (*BABAR* collaboration), Nucl. Instrum. Meth. A **726**, 203 (2013).
[15] D. J. Lange, Nucl. Instrum. Meth. A **462**, 152 (2001).
[16] S. Agostinelli *et al.* (GEANT4 Collaboration), Nucl. Instrum. Meth. A **506**, 250 (2003).
[17] B. Aubert *et al.* (*BABAR* Collaboration), Nucl. Instrum. Meth. A **479**, 1 (2002).
[18] B. Aubert *et al.* (*BABAR* Collaboration), Nucl. Instrum. Meth. A **729**, 2013 (615).
[19] Throughout this paper, all decay modes include the charge conjugated process.
[20] A. Drescher *et al.*, Nucl. Instrum. Meth. A **237**, 464 (1985).
[21] J.C. Anjos *et al.* (E691 Collaboration), Phys. Rev. D **48**, 56 (1993).
[22] G.C. Fox, S. Wolfram, Phys. Rev. Lett. **41**, 1581 (1978).
[23] H. Albrecht et al. (ARGUS Collaboration), Phys. Lett. B **241**, 278 (1990).